REPORT DOCUMENTATION PAGE

Form Approved OMB NO. 0704-0188

1. REPORT DATE (DD-MM-YYYY)	2. REPORT TYPE	3. DATES COVERED (From - To)
	New Reprint	-

4. TITLE AND SUBTITLE
Nanotwins in nanocrystalline Mg–Alalloys: an insight from high-resolutionTEM and molecular dynamics simulation

5a. CONTRACT NUMBER
W911NF-09-1-0558

5b. GRANT NUMBER

5c. PROGRAM ELEMENT NUMBER
611102

6. AUTHORS
M. Pozuelo, S.N. Mathaudhu, S. Kim, B. Li, W.H. Kao, J.-M. Yang

5d. PROJECT NUMBER

5e. TASK NUMBER

5f. WORK UNIT NUMBER

7. PERFORMING ORGANIZATION NAMES AND ADDRESSES
University of California - Los Angeles
Office of Contract and Grant Administration
11000 Kinross Avenue, Suite 211
Los Angeles, CA 90095 -1406

8. PERFORMING ORGANIZATION REPORT NUMBER

9. SPONSORING/MONITORING AGENCY NAME(S) AND ADDRESS (ES)
U.S. Army Research Office
P.O. Box 12211
Research Triangle Park, NC 27709-2211

10. SPONSOR/MONITOR'S ACRONYM(S)
ARO

11. SPONSOR/MONITOR'S REPORT NUMBER(S)
57244-EG.6

12. DISTRIBUTION AVAILIBILITY STATEMENT
Approved for public release; distribution is unlimited.

13. SUPPLEMENTARY NOTES
The views, opinions and/or findings contained in this report are those of the author(s) and should not contrued as an official Department of the Army position, policy or decision, unless so designated by other documentation.

14. ABSTRACT
Twinning in hexagonal close-packed Mg alloys has been reported to be unfavorable when the grain size is reduced below a couple of microns and suppressed at the nanoscale. Using high-resolution transmission electron microscopy, we present evidence of nanotwins (<1 nm) in nanocrystalline Mg – Al alloys processed by cryomilling. The commonly observed twinning modes for coarse-grained Mg are identi ? ed and supported with atomistic

15. SUBJECT TERMS
nanocrystalline Mg – Al alloys; nanotwins; cryomilling;transmission electron microscopy; molecular dynamics simulations

16. SECURITY CLASSIFICATION OF:			17. LIMITATION OF ABSTRACT	15. NUMBER OF PAGES	19a. NAME OF RESPONSIBLE PERSON
a. REPORT	b. ABSTRACT	c. THIS PAGE			Jenn-Ming Yang
UU	UU	UU	UU		19b. TELEPHONE NUMBER 310-825-2758

Report Title

Nanotwins in nanocrystalline Mg–Alalloys: an insight from high-resolutionTEM and molecular dynamics simulation

ABSTRACT

Twinning in hexagonal close-packed Mg alloys has been reported to be unfavorable when the grain size is reduced below a couple of microns and suppressed at the nanoscale. Using high-resolution transmission electron microscopy, we present evidence of nanotwins (<1 nm) in nanocrystalline Mg – Al alloys processed by cryomilling. The commonly observed twinning modes for coarse-grained Mg are identi ? ed and supported with atomistic molecular dynamics simulations. The speci ? c thermomechanical conditions offered by cryomilling facilitate the generation of deformation twins that are not observed with conventional deformation processing methods.

REPORT DOCUMENTATION PAGE (SF298)
(Continuation Sheet)

Continuation for Block 13

ARO Report Number 57244.6-EG
Nanotwins in nanocrystalline Mg–Alalloys: an in...

Block 13: Supplementary Note

Approved for public release; distribution is unlimited.

Philosophical Magazine Letters, 2013
Vol. 93, No. 11, 640–647, http://dx.doi.org/10.1080/09500839.2013.833353

Nanotwins in nanocrystalline Mg–Al alloys: an insight from high-resolution TEM and molecular dynamics simulation

M. Pozuelo[a]*, S.N. Mathaudhu[b], S. Kim[c], B. Li[c], W.H. Kao[d] and J.-M. Yang[a]

[a]*Department of Materials Science and Engineering, University of California Los Angeles, Los Angeles, CA 90095, USA;* [b]*Weapons and Materials Research Directorate, U.S. Army Research Laboratory, Aberdeen Proving Ground, Aberdeen, MD 21005, USA;* [c]*Center for Advanced Vehicular Systems, Mississippi State University, Mississippi State, MS 39762-5405, USA;* [d]*Institute for Technology Advancement, University of California Los Angeles, Los Angeles, CA 90095, USA*

(*Received 10 April 2013; accepted 5 August 2013*)

Twinning in hexagonal close-packed Mg alloys has been reported to be unfavorable when the grain size is reduced below a couple of microns and suppressed at the nanoscale. Using high-resolution transmission electron microscopy, we present evidence of nanotwins (<1 nm) in nanocrystalline Mg–Al alloys processed by cryomilling. The commonly observed twinning modes for coarse-grained Mg are identified and supported with atomistic molecular dynamics simulations. The specific thermomechanical conditions offered by cryomilling facilitate the generation of deformation twins that are not observed with conventional deformation processing methods.

Keywords: nanocrystalline Mg–Al alloys; nanotwins; cryomilling; transmission electron microscopy; molecular dynamics simulations

1. Introduction

Nanocrystalline (nc) metals are well known for their high strength, but frequently suffer significant losses in ductility due to the reduction in the work hardening potential. However, recent studies have shown that the introduction of nanotwins in nanocrystalline materials can result in an extraordinarily high strength with concurrent retention of ductility [1]. The ductility is retained via the movement of dislocations along the nanotwin boundaries, which effectively retains the work hardening potential unavailable to most 'conventional' nanograined materials. While such behavior has been observed for fcc and bcc materials, deformation twins are rarely observed in hcp nc Mg [2].

It has been reported that deformation twinning in nc Mg is suppressed due to the high stress required for a twin to nucleate [2], which increases drastically with decreasing grain size to the nanometer scale [3–5]. More explicitly, in hcp metals, dislocations on the non-close-packed pyramidal planes are much harder to be activated than those dislocations with a Burgers vector in the close-packed directions that are on the basal plane or prism planes [6,7]. Hence, profuse deformation twinning is activated in coarse-

*Corresponding author. Email: pozuelo@ucla.edu

grained hcp metals when loaded [8–10]. These deformation twins, which provide the dominant plastic deformation mechanism, strongly depend on temperature [3,11], strain rate [11,12], and grain size [11,13–17]. It has been reported that larger grain sizes are more favorable for twin nucleation [11,13–17]. This is attributed to the critical stress, σ, for dislocation slip and twinning that follows a Hall–Petch relationship $\sigma = \sigma_0 + kd^{-1/2}$, where σ_0 is the stress at very large grain sizes, k is the Hall–Petch slope, and d is the grain size. It is well known that by decreasing the grain size, the Hall–Petch slope for deformation twinning can be much larger than that for dislocation slip [11,14]. Therefore, a smaller average grain size will further hinder deformation by twinning if the critical stress to nucleate a twin is not reached.

It has recently been reported that by alloying Mg with Ti in a nc Mg–Ti alloy [18], with Y and Zn in $Mg_{97}Y_2Zn_1$ (wt.%) [19] prepared via room temperature mechanical milling, the energy path for twinning can change and the deformation twins can be observed. While these studies provide evidence of twinning in nc Mg alloys, they do not de-convolute the effect of alloying (to reduce the stacking fault energy for easier twin generation) from the thermomechanical processing conditions during mechanical milling which may induce deformation twins. Deformation twins in nanostructured AZ80 Mg alloy [20] have also been observed in powders produced by cryomilling, but no evaluation of the nature of the twinning modes was provided.

In this work, we expand on these results by systematically identifying the primary deformation twinning modes which occur in nc Mg–Al alloys during cryomilling. Using high-resolution transmission electron microscopy (HRTEM) concurrently with molecular dynamic (MD) simulations, it is demonstrated that twinning modes typical of coarse-grained Mg alloys, namely $\{1\,0\,\bar{1}\,1\}\langle 1\,0\,\bar{1}\,\bar{2}\rangle$ and $\{1\,0\,\bar{1}\,2\}\langle 1\,0\,\bar{1}\,\bar{1}\rangle$ type deformation twins, can be activated in nc Mg-based alloys. We postulate that the combination of high strain rate and low temperature plastic deformation during cryomilling facilitates the generation of nanotwins and represent a powerful method for property improvement in nc Mg alloys.

2. Experimental procedure

Commercially available gas-atomized Mg and Al alloy powders were blended to formulate two composition $Mg_{70}Al_{30}$ and $Mg_{90}Al_{10}$ (wt.%) alloys. The blended powder was cryogenically milled for 8 h under liquid nitrogen atmosphere in a Union Process, Szegvari mill at California Nanotechnologies Inc. HRTEM analysis was carried out using a FEI Titan TEM operating at 300 kV. TEM samples were prepared by spreading of an ultrasonicated suspension of the cryomilled powders in ethanol onto a regular Cu grid. HRTEM images were Fourier filtered to reduce the background noise using Image J. Atomistic simulations were carried out to study the deformation behavior of nc Mg upon tensile loading. Our simulations were performed with the LAMMPS [21], a parallel simulation code for systems with a large number of atoms. Many-body semi-empirical interatomic potential developed by Liu et al. [22] was used in our simulation. This EAM potential (embedded atom method) [23] fits to both experimental and *ab initio* data and describes the mechanical properties of Mg with satisfactory accuracy. A total of 27 grains were constructed by Voronoi tessellation procedures [24] and the crystal orientations were randomly assigned. The system contains about 10 million atoms in a 60 nm × 60 nm × 60 nm box. No periodic boundary conditions were applied

in all the three directions. The time step size was 1.0 fs. To make our conclusions more general, we performed our simulations at 300 K. Additionally, the extremely low temperature conditions during cryomilling were compensated with a high strain rate in our MD simulations. The deformation was performed such that the atoms on the right surface were moved at a constant displacement rate corresponding to a strain rate about 10^9 per second, while the atoms on the left surface were held still. Centro-symmetry parameter (CSP) [25] was used to identify the lattice defects such as twins, dislocations, and interfaces. In all the plots, atoms are colored according to their relative magnitude of the centro-symmetry parameter.

3. Results and discussion

Nearly equiaxed nc Mg grains have been obtained for both $Mg_{70}Al_{30}$ and $Mg_{90}Al_{10}$ cryomilled powders with an average grain size of 27 and 30 nm, respectively. Details of the processing and characterization of the cryomilled powders are described in detail in Ref. [26]. Figure 1 displays a detailed TEM analysis of $\{1\,0\,\bar{1}\,1\}$ twin boundaries (TBs) and their propagation within nc $Mg_{70}Al_{30}$ (top panel) and $Mg_{90}Al_{10}$ grains (bottom panel). $\{1\,0\,\bar{1}\,1\}$ TBs (highlighted by yellow solid lines) giving a mirror relationship between the parent and the twin planes can be observed in both HRTEM images of $Mg_{70}Al_{30}$ (Figure 1(a)) and $Mg_{90}Al_{10}$ grains (Figure 1(d)). It is interesting to observe that the TBs can propagate by the motion of atomic steps with a step height of two atomic $\{1\,0\,\bar{1}\,1\}$ planes (highlighted by two arrows parallel to the $\{1\,0\,\bar{1}\,1\}$ planes). Figure 1(b) is the fast Fourier transformation (FFT) of the image in (a). Its color-coded indexed FFT for clarity is shown in Figure 1(c). Interplanar distances measurements indicate that the misorientation relation between the parent (blue lattice/black in print) and the twin (red lattice/grey in print) is close to the expected angle of 58° for a grain oriented to the $\langle 1\,\bar{2}\,1\,\bar{3}\rangle$ zone axis. This angle is in good agreement with that previously reported [27,28] characteristic of rotational twins on $\{1\,0\,\bar{1}\,1\}$ planes. Note that $\pm(1\,\bar{1}\,0\,1)_T$ (planes from the twin) and $\pm(0\,\bar{1}\,1\,1)_P$ (planes from the parent) are almost parallel to each other.

Figure 1(d) is a HRTEM image showing nanotwins of only 0.8 nm widths in a nanocrystalline $Mg_{90}Al_{10}$ grain of around 6 nm size. Figure 1(e) is the FFT of the image. Its color-coded indexed FFT (Figure 1(f)) indicates that the nanocrystalline grain is oriented to the $\langle 1\,\bar{2}\,1\,\bar{3}\rangle$ zone axis. In addition to some extra spots from the neighboring grains, two reciprocal lattices sharing the same zone axis are detected. The red (grey in print) denotes the reciprocal lattice for the twin that is rotated by 58° with respect to the $\langle 0\,\bar{1}\,1\,1\rangle^*$ direction of the parent in blue (black in print). Again $\pm(1\,\bar{1}\,0\,1)$ planes from the twin and $\pm(0\,\bar{1}\,1\,1)$ from the parent are almost parallel to each other. As observed in the $Mg_{70}Al_{30}$ alloy, TBs can propagate by the motion of atomic steps with a step height of two atomic $\{1\,0\,\bar{1}\,1\}$ planes (Figure 1(d)). We provide further evidence using MD simulations (Figure 3(b)) that $\{1\,0\,\bar{1}\,1\}\langle 1\,0\,\bar{1}\,\bar{2}\rangle$ contraction twins can be activated in nc Mg grains and controlled by two-layer zonal twinning dislocations [29,30].

In addition to contraction twins, we have also observed extension twinning on the characteristic $\{1\,0\,\bar{1}\,2\}$ planes. $\{1\,0\,\bar{1}\,2\}\langle 1\,0\,\bar{1}\,\bar{1}\rangle$ extension twin is a common deformation twinning mode seen in coarse-grained Mg [31–33] and in many other hcp systems [34]. Figure 2 shows a HRTEM image of several nc $Mg_{70}Al_{30}$ grains. From the two

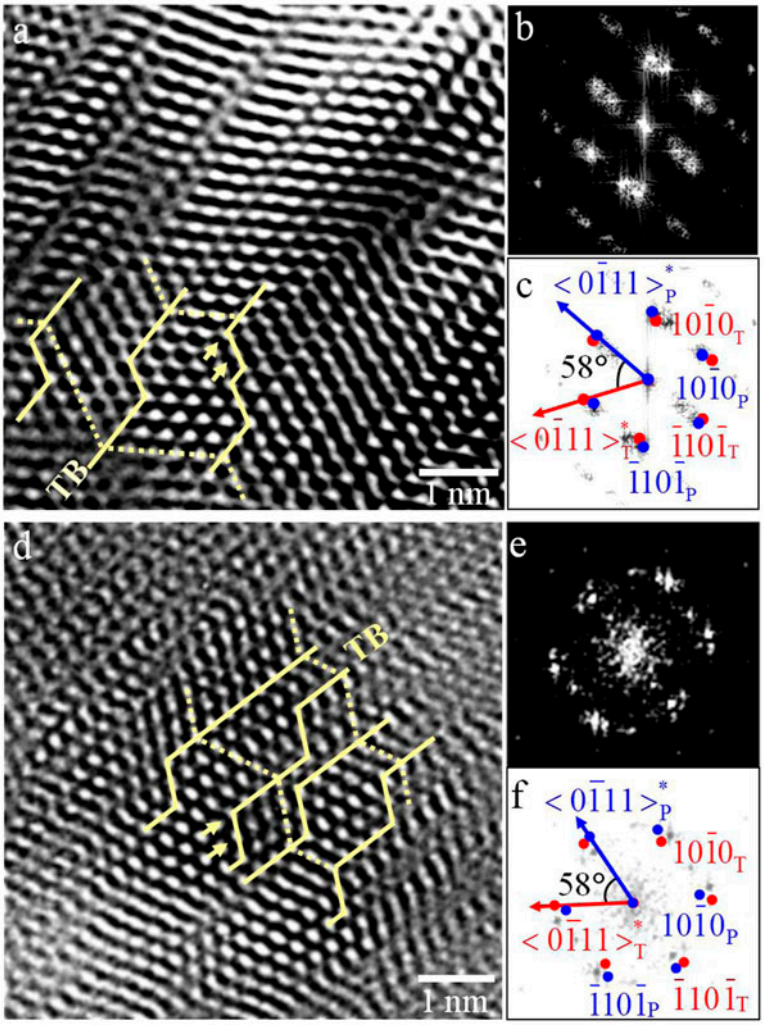

Figure 1. (colour online). (a) HRTEM image of a nanocrystalline $Mg_{70}Al_{30}$ grain showing $\{1\,0\,\bar{1}\,1\}$ twin boundaries (TBs). (b) Fast Fourier transform (FFT) of the image. (c) Color-coded indexed FFT showing the misorientation relation between the parent (blue/black in print) and the twin (red/grey in print) close to 58°. (d) HRTEM image of a nanocrystalline $Mg_{90}Al_{10}$ grain showing $\{1\,0\,\bar{1}\,1\}$ TBs. (e) FFT of the image. (f) Color-coded indexed FFT showing the characteristic relation between the parent (blue/black in print) and the twin (red/grey in print) close to 58°.

FFTs (inset) labelled as *P* and *T* from the parent and twin regions located at both sides of the TB, we identify the $\langle 1\,0\,\bar{1}\,2\rangle^*$ direction that has been highlighted by dashed yellow lines in both FFTs. From the indexed FFTs, in addition to some extra spots from the neighboring grains, we can at least identify $(0\,0\,0\,2)_P$ and $(0\,1\,\bar{1}\,2)_P$ planes from the parent that have been rotated 86° (as expected) with respect to the $\langle 1\,0\,\bar{1}\,2\rangle^*$ direction to result in $(0\,0\,0\,2)_T$ and $(0\,1\,\bar{1}\,2)_T$. Figure 2(b) is a HRTEM image of the region

highlighted by the rectangle in which $\{10\bar{1}2\}$ TB and (0001) basal planes are marked. As expected, the basal planes of the parent and the twin appear nearly perpendicular to each other.

TEM results provide evidence that nanotwins can be activated in two different nc Mg–Al alloys processed under the same cryomilling conditions. These results suggest a strong correlation between cryomilling and twinning in hcp nc Mg-alloys. During cryomilling, the development of nanostructures is mainly accomplished via the formation of shear bands under localized deformation [35]. The milling time required to attain nc grains is significantly reduced because the extremely low temperature suppresses the annihilation of dislocations [36–37]. As the plastic deformation increases, under high strain rate and cryogenic temperatures, the number of dislocations becomes larger. We believe that the high dislocation density on the grain boundaries (GBs) leads to a higher localized stress that might act as the driving force for twins' nucleation.

MD simulations were performed in order to support our experimental observations. The atomistic simulations are based on pure nanocrystalline Mg under high strain rate conditions. This setting is expected to be less favorable to twin formation as compared to Mg–Al alloys. As a matter of fact, it has recently been reported by density functional theory calculations [38,39] that Al could be included in the group of those elements that decrease or do not change the value of the stacking fault energy of pure Mg. The initial configuration of our simulation is shown as an inset in Figure 3(a). Atoms residing at GBs and surfaces have different CSP values than those in perfect lattice points. As the strain increases, dislocation slip and deformation twinning are activated. Figure 3(a) shows a top view of a thin slice of the system that is parallel to the top surface at time step 80 ps. A partial dislocation and the associated stacking faults (SFs) are presented in blue (dark in print). Dislocations are always nucleated from GBs and free surfaces, and propagate across the grains. Deformation twins can be seen in the top and lower right regions. Twins are nucleated at GBs or triple junctions of the GBs. Enlarged views of twins and SFs are shown in Figure 3(b) and (c).

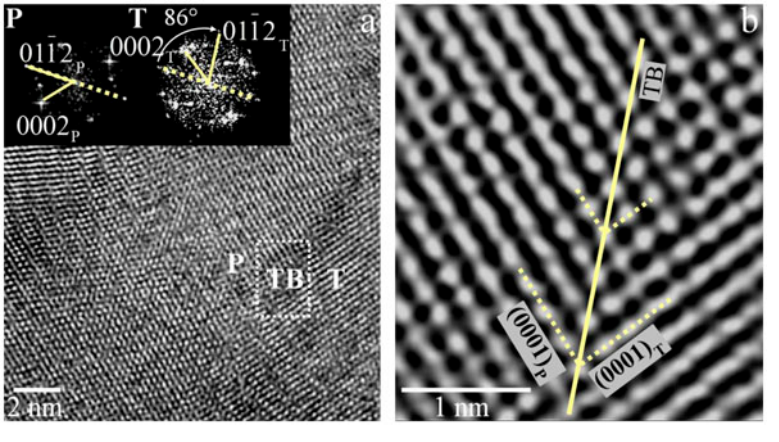

Figure 2. (colour online). (a) HRTEM image of several nanocrystalline $Mg_{70}Al_{30}$ grains showing a $\{10\bar{1}2\}$ TB highlighted by the rectangle. Insets are FFTs of the parent (P) and the twin (T) showing the characteristic rotational angle of 86°. (b) Atomic-resolved image of the $\{10\bar{1}2\}$ TB from the region highlighted by the rectangle in (a).

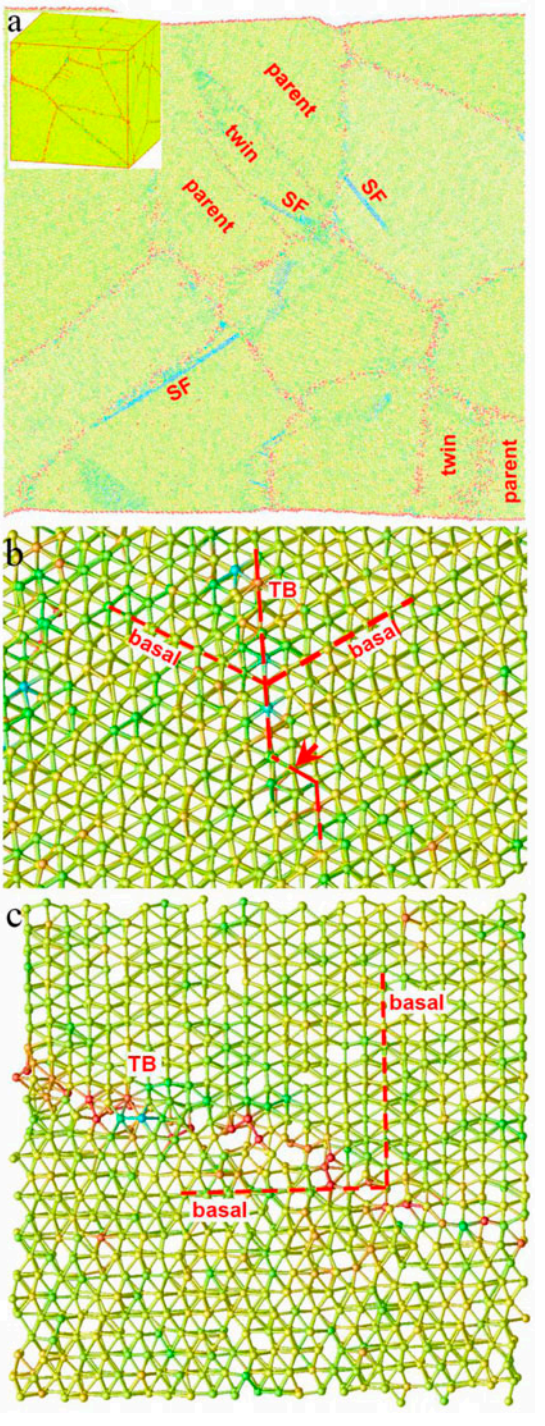

Figure 3. (colour online). (a) Cross-sectional view of the grains (20 nm in size) of a thin slice parallel to the figure plane from the initial configuration of nanocrystalline Mg (inset). (b) $\{1\,0\,\bar{1}\,1\}\langle 1\,0\,\bar{1}\,\bar{2}\rangle$ contraction twins from the top middle grain in (a). A two-layer zonal dislocation that controls the migration of the twin boundary is highlighted by an arrow. (c) $\{1\,0\,\bar{1}\,2\}\langle 1\,0\,\bar{1}\,\bar{1}\rangle$ extension twins from the bottom right grain in (a).

To identify the twinning modes, we tilted the lattices meticulously such that twinning elements, that is, the twinning plane and the plane of shear can be well defined. For the two most commonly observed twinning modes, that is, $\{1\,0\,\bar{1}\,2\}\langle 1\,0\,\bar{1}\,\bar{1}\rangle$ extension and $\{1\,0\,\bar{1}\,1\}\langle 1\,0\,\bar{1}\,\bar{2}\rangle$ contraction twins, we tilted the system such that the basal planes of the parent and the twin and the twinning plane are all perpendicular to the figure plane. The shear plane is exactly parallel to the figure plane and the zone axis is parallel to $\langle 1\,\bar{2}\,1\,0\rangle$. Figure 3(b) shows a $\{1\,0\,\bar{1}\,1\}\langle 1\,0\,\bar{1}\,\bar{2}\rangle$ contraction twin where the mirror symmetry is well defined. A two-layer zonal twinning dislocation [29,30] can be identified, which controls the migration of TB as observed experimentally in Figure 1. The experimentally observed $\{1\,0\,\bar{1}\,2\}\langle 1\,0\,\bar{1}\,\bar{1}\rangle$ extension twin was also validated with our simulations in Figure 3c. As expected, twin and parent lattices satisfy the twin orientation relationship nearly perpendicular to each other.

4. Summary

We propose a comprehensive approach based on high-resolution TEM studies and MD simulations to demonstrate the formation of nanotwins in nanocrystalline Mg-Al alloys. We present the evidence of narrow (<1 nm) deformation twins in two nanocrystalline magnesium alloys ($Mg_{70}Al_{30}$ and $Mg_{90}Al_{10}$ wt.%) processed under the same cryomilling conditions. We demonstrate that the two common $\{1\,0\,\bar{1}\,1\}\langle 1\,0\,\bar{1}\,\bar{2}\rangle$ and $\{1\,0\,\bar{1}\,2\}\langle 1\,0\,\bar{1}\,\bar{1}\rangle$ twinning systems in coarse-grained Mg are prevalent in nanocrystalline grains. Our results suggest cryomilling as an optimum severe plastic deformation technique that provides high stress to activate the deformation twins in nanocrystalline Mg grains.

Acknowledgements

The authors express their appreciation to the Army Research Office for financial support of this work under the ARO Contract No. W911NF-09-1-0558. They are particularly grateful to the ARO program manager, Dr Larry Russell and to Christopher Melnyk for his assistance with the cryomilling performed at California Nanotechnologies Inc.

References

[1] K. Lu, L. Lu and S. Suresh, Science 324 (2009) p. 349.
[2] H.J. Choi, Y. Kim, J.H. Shin and D.H. Bae, Mater. Sci. Eng., A 527 (2010) p. 1565.
[3] M.R. Barnett, Z. Keshavarz, A.G. Beer and D. Atwell, Acta Mater. 52 (2004) p. 5093.
[4] J.A. Venables, J. Phys. Chem. Solids 25 (1964) p. 693.
[5] V. Yamakov, D. Wolf, S.R. Phillpot and H. Gleiter, Acta Mater. 50 (2002) p. 5005.
[6] L. Wen, P. Chen, Z.-F. Tong, B.-Y. Tang, L.-M. Peng and W.-J. Ding, Eur. Phys. J. B72 (2009) p. 397.
[7] J. Koike, T. Kobayashi, T. Mukai, H. Watanabe, M. Suzuki, K. Maruyama and K. Higashi, Acta Mater. 51 (2003) p. 2055.
[8] R.E. Reed-Hill and W.D. Robertson, Acta Metall. 5 (1957) p. 717.
[9] O. Muránsky, M.R. Barnett, D.G. Carr, S.C. Vogel and E.C. Oliver, Acta Mater. 58 (2010) p. 1503.
[10] Y. Wang, L.Q. Chen, Z.K. Liu and S.N. Mathaudhu, Scr. Mater. 62 (2010) p. 646.
[11] M.A. Meyers, O. Vöhringer and V.A. Lubarda, Acta Mater. 49 (2001) p. 4025.

[12] J.W. Christian and S. Mahajan, Prog. Mater Sci. 39 (1995) p. 1.
[13] Q. Yang and A.K. Ghosh, Acta Mater. 54 (2006) p. 5159.
[14] M.R. Barnett, Scr. Mater. 59 (2008) p. 696.
[15] Q. Yang and A.K. Ghosh, Acta Mater. 54 (2006) p. 5147.
[16] H.H. Fu, D.J. Benson and M.A. Meyers, Acta Mater. 49 (2001) p. 2567.
[17] Y.T. Zhu, X.Z. Liao and X.L. Wu, Prog. Mater Sci. 57 (2012) p. 1.
[18] X.L. Wu, K.M. Youssef, C.C. Koch, S.N. Mathaudhu, L.J. Kecskés and Y.T. Zhu, Scr. Mater. 64 (2011) p. 213.
[19] K.M. Youssef, Y.B. Wang, X.Z. Liao, S.N. Mathaudhu, L.J. Kecskés, Y.T. Zhu and C.C. Koch, Mater. Sci. Eng., A 528 (2011) p. 7494.
[20] B. Zheng, O. Ertorer, Y. Li, Y. Zhou, S.N. Mathaudhu, C.Y.A. Tsao and E.J. Lavernia, Mater. Sci. Eng. A528 (2011) p. 2180.
[21] S. Plimpton, J. Comput. Phys. 117 (1995) p. 1.
[22] X.-Y. Liu, J.B. Adams, F. Ercolessi and J.A. Moriarty, Model. Simul. Mater. Sci. Eng. 4 (1996) p. 293.
[23] S.M. Foiles, M.I. Baskes and M.S. Daw, Phys. Rev. B 33 (1986) p. 7983.
[24] G. Voronoi and J. Reine Angew, Math. 134 (1908) p. 198.
[25] C.L. Kelchner, S.J. Plimpton and J.C. Hamilton, Phys. Rev. B 58 (1998) p. 11085.
[26] M. Pozuelo, C. Melnyk, W.H. Kao and J.-M. Yang, J. Mater. Res. 26 (2011) p. 904.
[27] J. Wang, I.J. Beyerlein and C.N. Tomé, Scr. Mater. 63 (2010) p. 741.
[28] D.H. Kim, M.V. Manuel, F. Ebrahimi, J.S. Tulenko and S.R. Phillpot, Acta Mater. 58 (2010) p. 6217.
[29] B. Li and E. Ma, Acta Mater. 57 (2009) p. 1734.
[30] J. Wang, I.J. Beyerlein, J.P. Hirth and C.N. Tomé, Acta Mater. 59 (2011) p. 3990.
[31] I.J. Beyerlein, L. Capolungo, P.E. Marshall, R.J. McCabe and C.N. Tomé, Phil. Mag. 16 (2010) p. 2161.
[32] S.-G. Hong, S.H. Park and C.S. Lee, Acta Mater. 58 (2010) p. 5873.
[33] S.-G. Hong, S.H. Park and C.S. Lee, Scr. Mater. 64 (2011) p. 145.
[34] L. Zhang and Y. Han, Mater. Sci. Eng., A 523 (2009) p. 130.
[35] H.-J. Fecht, Nanostruct. Mater. 6 (1995) p. 33.
[36] E.J. Lavernia, B.Q. Han and J.M. Schoenung, Mater. Sci. Eng., A 493 (2008) p. 207.
[37] D.B. Witkin and E.J. Lavernia, Prog. Mater Sci. 51 (2006) p. 1.
[38] J. Han, X.M. Su, Z.-H. Jin and Y.T. Zhu, Scr. Mater. 64 (2011) p. 693.
[39] M. Muzyk, Z. Pakiela and K.J. Kurzydlowski, Scr. Mater. 66 (2012) p. 219.